

RESEARCH ARTICLE | NOVEMBER 20 2024

# Direct laser poling of lithium niobate on insulator with femtosecond laser

Tianxiang Xu; Feng Chen ; Wieslaw Krolikowski; Ady Arie ; Yan Sheng  



*Appl. Phys. Lett.* 125, 212902 (2024)

<https://doi.org/10.1063/5.0235673>



## Articles You May Be Interested In

Optimizing the efficiency of a periodically poled LNOI waveguide using *in situ* monitoring of the ferroelectric domains

*Appl. Phys. Lett.* (March 2020)

Domain structure formation by local switching in the ion sliced lithium niobate thin films

*Appl. Phys. Lett.* (April 2020)

Research progress of second-order nonlinear optical effects based on lithium niobate on insulator waveguides

*AIP Conf. Proc.* (November 2023)

21 November 2024 19:53:41

# Direct laser poling of lithium niobate on insulator with femtosecond laser

Cite as: Appl. Phys. Lett. **125**, 212902 (2024); doi: [10.1063/5.0235673](https://doi.org/10.1063/5.0235673)

Submitted: 29 August 2024 · Accepted: 9 November 2024 ·

Published Online: 20 November 2024



View Online



Export Citation



CrossMark

Tianxiang Xu,<sup>1</sup> Feng Chen,<sup>2</sup>  Wieslaw Krolikowski,<sup>3</sup> Ady Arie,<sup>4</sup>  and Yan Sheng<sup>1,a)</sup> 

## AFFILIATIONS

<sup>1</sup>Laboratory of Infrared Materials and Devices, Research Institute of Advanced Technologies, Zhejiang Key Laboratory of Advanced Optical Functional Materials and Devices, Ningbo University, Ningbo, Zhejiang 315211, China

<sup>2</sup>School of Physics, Shandong University, Jinan, China

<sup>3</sup>Department of Quantum Science and Technology, Research School of Physics, Australian National University, Canberra, ACT 2601, Australia

<sup>4</sup>School of Electrical Engineering, Fleischman Faculty of Engineering, Tel Aviv University, Tel Aviv-Yafo 69978, Israel

<sup>a)</sup> Author to whom correspondence should be addressed: [shengyan@nbu.edu.cn](mailto:shengyan@nbu.edu.cn)

## ABSTRACT

We demonstrated experimentally direct femtosecond writing of ferroelectric domains in lithium niobate on insulator. The fabricated ferroelectric domain structures were characterized using Cherenkov second harmonic microscopy and piezoresponse force microscopy. We also experimentally explored the far-field second harmonic generation from the laser-induced ferroelectric domain structures. This study opens the door for direct laser writing of lithium niobate-based integrated photonic circuits, which typically require on-chip frequency conversion and wavefront control.

Published under an exclusive license by AIP Publishing. <https://doi.org/10.1063/5.0235673>

Recently, lithium niobate on insulator (LNOI) has attracted significant attention due to its potential in integrated photonics.<sup>1–5</sup> With its excellent material properties inherited from single-crystal lithium niobate (LiNbO<sub>3</sub>) and the strong light confinement in the nanoscale thin film, LNOI-based microresonators, metasurface, and domain-engineered microstructures have been developed for high-speed electro-optic modulators, acousto-optic devices, and ultra-efficient nonlinear frequency converters.<sup>6–10</sup> These functions are crucial for shaping the future of optical networks and communications.

Many potential applications of LNOI rely on ferroelectric domain engineering, which provides a unique way to modulate the second-order nonlinear coefficient for quasi-phase matching frequency conversion and nonlinear wavefront shaping.<sup>11–14</sup> Currently, ferroelectric domain engineering in LNOI is achieved through the interaction of an external electric field applied along the ferroelectric  $z$  axis of the LiNbO<sub>3</sub> crystal.<sup>15</sup> This process, known as electric field poling, typically requires a much higher electric field for thin films compared to bulk crystals. The electric field can be applied via the tip of an atomic force microscopy (AFM),<sup>16–19</sup> resulting in inverted domain structures of limited dimensions due to the small scan range of commercial AFMs. More commonly, periodic electrodes patterned on the surfaces of LNOI wafer are used to pole ferroelectric domains in both  $z$ -cut and

$x$ -cut LNOI thin films.<sup>15,20,21</sup> However, this electric approach generally requires several nano-fabrication steps of resist deposition, development, liftoff, and metal evaporation or sputtering. It is not favorable for low-loss optical waveguide applications due to the presence of patterned metal electrodes near the optical mode. Special measures have been taken to reach sub-micron poling periods with this electric method, such as careful selection of the poling parameters including the poling pulse waveform and amplitude.<sup>22</sup>

It has been demonstrated that all-optical poling with tightly focused infrared femtosecond laser pulses can induce ferroelectric domain inversion in bulk lithium niobate, barium calcium titanate, strontium barium niobate, calcium barium niobate, and relaxor-PbTiO<sub>3</sub> crystals.<sup>23,24</sup> This infrared method relies on nonlinear absorption of light in the optical beam's focal volume, which induces a high temperature gradient, and the appearance of a thermoelectric field that locally inverts the direction of the spontaneous polarization. The method can form three-dimensional ferroelectric domain structures,<sup>25–27</sup> applies to different crystallographic orientations, and offers spatial resolution on the sub-micrometer scale. While the advantages of infrared laser poling have been confirmed in bulk ferroelectric crystals, its validity and performance in poling ferroelectric thin film remain unknown.

In this Letter, we present an experimental study on the periodic poling of LNOI thin film using tightly focused infrared femtosecond pulses. The light-induced ferroelectric domains' structures are characterized using piezoresponse force microscopy (PFM) and Cherenkov second harmonic microscopy. We experimentally investigate the influences of the writing laser wavelength and laser power on domain inversion. The second harmonic generated from the laser-induced ferroelectric domains is also studied. This work introduces an all-optical method for domain engineering in ferroelectric thin films, which is useful for the construction of integrated photonic devices for the next generation of optical networks and communications.

The *z*-cut LNOI thin film used in this work was obtained from a commercial source (NanoLN, Jinan Jingzheng Electronics Co., Ltd.). It consists of three layers (from top to bottom): a single-domain congruent LiNbO<sub>3</sub> thin film with a thickness of 3 μm, a SiO<sub>2</sub> buffer layer with a thickness of 2 μm, and a congruent LiNbO<sub>3</sub> bulk substrate with a thickness of 500 μm. The thickness of the LiNbO<sub>3</sub> films used in this study is greater than the typical 700–900 nm range. This demonstrates that thicker films can be poled without the use of an electric field and may offer advantages, such as handling higher power in waveguide configurations. The femtosecond-laser-induced domain inversion was conducted using a Ti:sapphire femtosecond oscillator (Chameleon, Coherent). The laser wavelength was tunable in the range of 680–1080 nm, with a pulse duration of 180 fs and a repetition rate of 76 MHz. As shown in Fig. 1, the laser beam propagated along the *z*-axis of the LNOI thin film, with its polarization and power adjustable using a combination of a half wave plate and a polarizer. The beam was focused with an objective lens [50×, Numerical aperture (NA) 0.65], resulting in an estimated beam waist of about 1 μm. The LNOI sample was fixed on a translational stage that could automatically move along three axes, and the *-z* surface of the film was exposed to laser beam. A mechanical shutter controlled by computer was used to adjust the exposure time.

In the experiment, by scanning the laser focus within the plane of the thin film, the desired inverted domain structures can be fabricated. For example, Fig. 2 shows the square and hexagonal lattice inverted domain structures with a period of 2 μm. The writing laser wavelength was 720 nm, and the power was 190 mW. Hence, the corresponding peak intensity was  $1.8 \times 10^{12}$  W/cm<sup>2</sup>. For each domain inversion, the shutter was on for 0.5 s. These images were obtained using Cherenkov

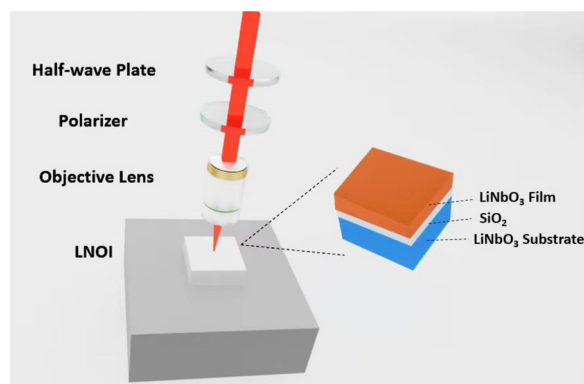


FIG. 1. A schematic diagram for all-optical poling of LiNbO<sub>3</sub> thin film using tightly focused femtosecond infrared pulses.

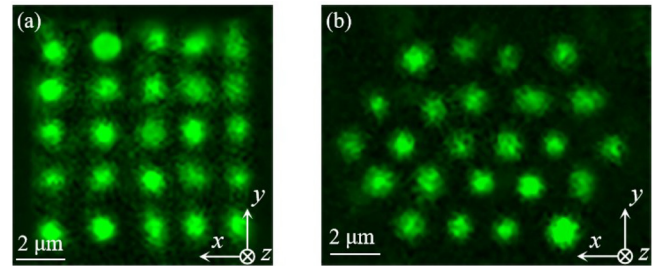


FIG. 2. The nonlinear optical microscopic images of the inverted ferroelectric domains induced by femtosecond laser in the LNOI thin film. (a) The square lattice and the (b) hexagonal lattice of domains.

second harmonic microscopy,<sup>28</sup> which is based on the principle that the Cherenkov second harmonic signal is enhanced at the ferroelectric domain walls.<sup>29</sup> By recording the second harmonic signals at various spatial positions, we obtained the distribution of the ferroelectric domain walls. The key to this imaging technique is that the incident laser spot must be small enough to cover only a single-domain wall.

We also used piezoelectric force microscopy (PFM) to characterize the ferroelectric domain inversion induced by the femtosecond beam. For this purpose, we prepared a periodic square ferroelectric domain structure with a period of 2 μm, and the resulting PFM phase images are shown in Fig. 3. It is evident that, indeed, ferroelectric domain inversion in the thin film of LiNbO<sub>3</sub> has been achieved.

Additionally, we observed second harmonic generation (SHG) from the laser-written inverted domain structures. As illustrated in Fig. 4(a), the fundamental laser beam in this experiment was incident along *z*-axis of the thin film, and the emitted second harmonic beam was projected on a screen behind the sample and recorded by a CCD camera. Figure 4(b) shows the second harmonic patterns observed when the incident laser beam (wavelength 950 nm) was focused through an objective lens with NA = 0.3. Two second harmonic rings were observed. The inner (outer) ring was radially (azimuthally) polarized. Based on the symmetry of lithium niobate, these results indicate that the emissions of the inner and outer rings were governed by O<sub>1</sub>O<sub>1</sub>-E<sub>2</sub> and O<sub>1</sub>O<sub>1</sub>-O<sub>2</sub> interactions, respectively. We measured the

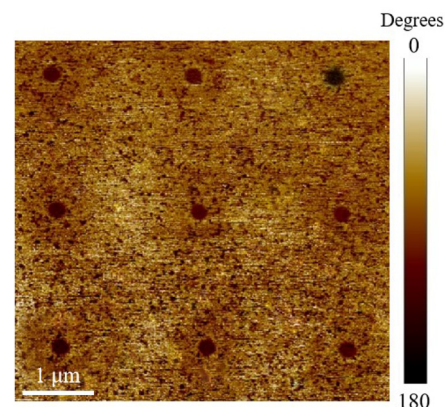
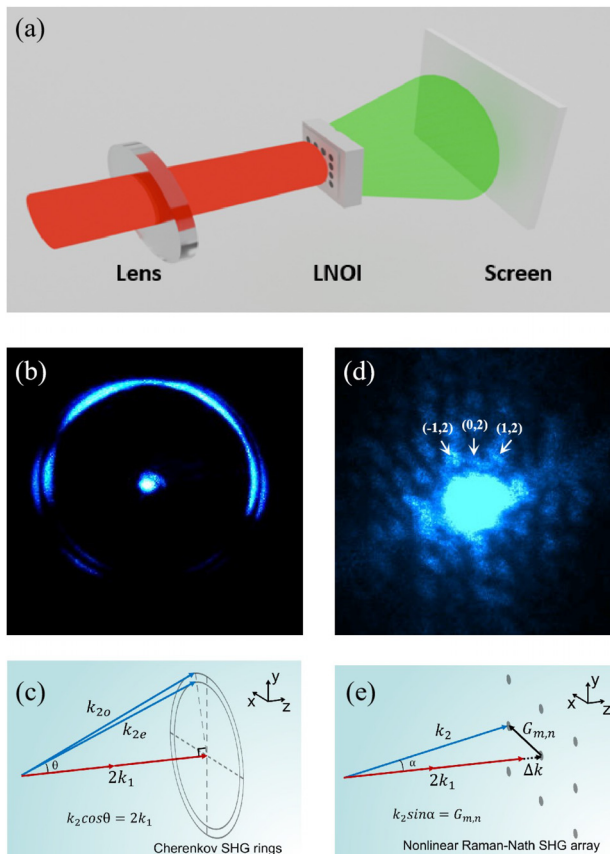


FIG. 3. The PFM phase image showing a square lattice of laser-induced inverted domains.



**FIG. 4.** (a) The experimental set up for second harmonic generation in optically poled LiNbO<sub>3</sub> thin films. (b) The recorded Cherenkov second harmonic rings at a fundamental wavelength of 950 nm. (c) The phase matching diagram of the Cherenkov second harmonic generation. (d) The second harmonic generation from the Nonlinear Raman-Nath diffraction. (e) The phase matching diagram of the Nonlinear Raman-Nath diffraction.

emission angles of the second harmonic rings and confirmed they represented the Cherenkov second harmonic emissions.<sup>30</sup> The Cherenkov angle is defined by the longitudinal phase matching condition  $k_2 \cos \theta = 2k_1$ , as shown in Fig. 4(c), with  $k_1$  and  $k_2$  being the wave vectors of fundamental and second harmonic beams, respectively. The measured external angle for the internal second harmonic ring was 44.42°, and that of the external ring was 47.79° at the fundamental wavelength of 950 nm, agreeing well with the calculated Cherenkov second harmonic angles of 44.97° and 47.40°, respectively. The experimental and calculated emission angles of the second harmonics are listed in Table I for all the experimental wavelengths: 850, 900, 950, 1000, and 1050 nm. Good agreement between the experimental values and theoretical predictions is clearly seen. The sixfold intensity modulations of the second harmonic rings result from the angular dependence of effective nonlinear coefficient in LiNbO<sub>3</sub> crystal.<sup>30</sup>

In addition to observing the Cherenkov second harmonic rings, we also detected the so-called Raman-Nath nonlinear diffraction.<sup>31</sup> In this experiment, we used a square array of inverted domains with a period of 15 μm, and the fundamental beam was focused with an

**TABLE I.** The experimental and calculated external emission angles for Cherenkov second harmonic rings in the LiNbO<sub>3</sub> thin film at different wavelengths.

$\lambda$ (nm) <sup>a</sup>	Inner ring (°)		Outer ring (°)	
	Experiment	Calculation	Experiment	Calculation
850	54.80	54.64	58.77	58.37
900	49.67	49.14	52.43	52.06
950	44.42	44.97	47.79	47.40
1000	41.67	41.65	44.46	43.76
1050	39.08	38.93	41.55	40.81

<sup>a</sup>The wavelength of incident fundamental beam.

objective lens with NA = 0.1. The relatively loose focusing allowed the beam to illuminate a greater number of domain structures, thereby engaging more periodicities that favor nonlinear Raman-Nath diffraction.<sup>31</sup> As illustrated in Fig. 4(d), the resulting second harmonic spots from the nonlinear Raman-Nath diffraction form a square lattice in the far field. In fact, the nonlinear Raman-Nath diffraction fulfills only the transverse phase matching condition, i.e.,  $k_2 \sin \alpha = G_{m,n}$ , as shown in Fig. 4(e). The measured emission angles for the (-1,2)-, (0,2)-, and (1,2)-order second harmonic diffractions are 4.02°, 3.46°, and 4.10°, respectively, which align closely with the calculated angles (4.06°, 3.63°, and 4.06°).<sup>31</sup>

In experiment, the inverted domain structures were written with laser wavelengths in the range of 720–800 nm, but no domain inversion was observed when the wavelength exceeded 800 nm. We observed that the laser wavelength range for domain inversion in the thin film is narrower than the range reported for the bulk crystals.

We also found that there is an optimal power range for femtosecond laser domains inversion in the thin film. When the laser power is too low, it is insufficient to induce domain inversion, but when the power is too high, the thin film approaches the threshold for optical damage, which is also detrimental to the formation of high-quality inverted domains. In our experiments, ferroelectric domain inversion was observed under laser powers ranging from 170 to 230 mW, with the highest probability of domain inversion occurring around 190 mW. The laser power used for optical poling of bulk lithium niobate was about 300 mW at the writing wavelength of 800 nm.<sup>23</sup> It seems that the threshold laser power required for spontaneous polarization inversion in the thin film is not higher than that in the bulk crystals. Table II lists the typical writing parameters used for laser poling in LiNbO<sub>3</sub> thin film and bulk crystals.

In conclusion, by using femtosecond laser direct-writing technique, we achieved all-optical ferroelectric domain inversion in lithium

**TABLE II.** Parameters used for laser poling in LNOI and LiNbO<sub>3</sub> bulk crystals.

	LNOI (this work)	LiNbO <sub>3</sub> <sup>23</sup>	MgO:LiNbO <sub>3</sub> <sup>32</sup>
Orientation	z-Cut	z-Cut	x-Cut
Wavelength (nm)	720	800	800
Pulse duration (fs)	180	180	75
Repetition rate (MHz)	76	76	80
Power (mW)	170-230	300	160

niobate thin films on isolator. Through Cherenkov second harmonic microscopy and piezoelectric atomic force microscopy, we confirmed the formation of high-quality inverted domain structures in the thin film. We also studied the second harmonic generation phenomena in the laser-fabricated inverted domain thin films and observed Cherenkov second harmonics and nonlinear diffractions consistent with theoretical predictions. Our research contributes toward the development of integrated lithium niobate thin films, particularly for on-chip nonlinear optical frequency conversion and beam shaping applications based on periodic domain structures. Future research directions could involve the formation of channel waveguides either before or after optical poling as well as extending all-optical poling to materials beyond LiNbO<sub>3</sub> thin films. Using all-optically poled LiNbO<sub>3</sub> thin films for nonlinear beam shaping is particularly intriguing. This could include forming nonlinear cylindrical lenses, generating Hermite-Gauss beams, and producing shaped entangled photons through spontaneous parametric downconversion.<sup>33</sup>

We wish to acknowledge the financial support of National Natural Science Foundation of China under Grant Nos. 62275136, 12274248, 11974196, and 12361141815, the National Key Research and Development Program of China (Grant No. 2019YFA0705000), the Natural Science Foundation of Zhejiang Province (LY22F050009), Australian Research Council, Israel Science Foundation (Grant No. 3117/23), and K C Wong Magna Fund of Ningbo University. We also acknowledge the technical support of Center for Advanced Microscopy, Australian National University.

## AUTHOR DECLARATIONS

### Conflict of Interest

The authors have no conflicts to disclose.

### Author Contributions

**Tianxiang Xu:** Investigation (lead). **Feng Chen:** Supervision (equal). **Wieslaw Krolikowski:** Supervision (equal). **Ady Arie:** Supervision (equal). **Yan Sheng:** Writing – original draft (lead).

### DATA AVAILABILITY

The data that support the findings of this study are available within the article. Raw data that support the findings of this study are available from the corresponding author upon reasonable request.

## REFERENCES

- A. Boes, B. Corcoran, L. Chang, J. Bowers, and A. Mitchell, "Status and potential of lithium niobate on insulator (LNOI) for photonic integrated circuits," *Laser Photonics Rev.* **12**, 1700256 (2018).
- D. Sun, Y. Zhang, D. Wang, W. Song, X. Liu, J. Pang, D. Geng, Y. Sang, and H. Liu, "Microstructure and domain engineering of lithium niobate crystal films for integrated photonic applications," *Light Sci. Appl.* **9**, 197 (2020).
- R. Ge, J. Wu, X. Liu, Y. Chen, and X. Chen, "Recent progress in thin-film lithium niobate photonic crystal," *Chin. Opt. Lett.* **88**, 445 (1983).
- Z. Xie, F. Bo, J. Lin, H. Hu, X. Cai, X. Tian, Z. Fang, J. Chen, M. Wang, F. Chen, Y. Cheng, and S. Zhu, "Recent development in integrated lithium niobate photonics," *Adv. Phys.: X* **9**(1), 2322739 (2024).
- Y. Jia, J. Wu, X. Sun, X. Yan, R. Xie, L. Wang, Y. Chen, and F. Chen, "Integrated photonics based on rare-earth ion doped thin-film lithium niobate," *Laser Photonics Rev.* **16**, 220059 (2022).
- R. R. Xie, G. Q. Li, F. Chen, and G. L. Long, "Microresonators in lithium niobate thin films," *Adv. Opt. Mater.* **9**(19), 2100539 (2021).
- J. Ma, F. Xie, W. Chen, J. Chen, W. Wu, W. Liu, Y. Chen, W. Cai, M. Ren, and J. Xu, "Nonlinear lithium niobate metasurfaces for second harmonic generation," *Laser Photonics Rev.* **15**(5), 2000521 (2021).
- J. Lu, J. B. Surya, X. Liu, A. W. Bruch, Z. Gong, Y. Xu, and H. X. Tang, "Periodically poled thin-film lithium niobate microring resonators with a second-harmonic generation efficiency of 250,000 %/w," *Optica* **6**, 1455 (2019).
- L. Ge, Y. Chen, H. Jiang, G. Li, B. Zhu, Y. A. Liu, and X. Chen, "Broadband quasi-phase matching in a MGO: PPLN thin film," *Photonics Res.* **6**, 954 (2018).
- Y. Jia, L. Wang, and F. Chen, "Ion-cut lithium niobate on insulator technology: Recent advances and perspectives," *Appl. Phys. Rev.* **8**, 011307 (2021).
- J. A. Armstrong, N. Bloembergen, J. Ducuing, and P. S. Pershan, "Interactions between light waves in a nonlinear dielectric," *Phys. Rev.* **127**, 1918–1939 (1962).
- S. Liu, K. Switkowski, C. Xu, J. Tian, B. Wang, P. Lu, W. Krolikowski, and Y. Sheng, "Nonlinear wavefront shaping with optically induced three-dimensional nonlinear photonic crystals," *Nat. Commun.* **10**, 3208 (2019).
- D. Wei, C. Wang, X. Xu, H. Wang, Y. Hu, Y. Zhu, C. Xin, X. Hu, Y. Zhang, D. Wu, J. Chu, S. Zhu, and M. Xiao, "Efficient nonlinear beam shaping in three-dimensional lithium niobate nonlinear photonic crystals," *Nat. Commun.* **10**, 4193 (2019).
- A. Shapira, L. Naor, and A. Arie, "Nonlinear optical holograms for spatial and spectral shaping of light waves," *Sci. Bull.* **60**, 1403–1415 (2015).
- J. Zhao, M. Rüsing, M. Roper, L. M. Eng, and S. Mookherjee, "Poling thin-film x-cut lithium niobate for quasi-phase matching with sub-micrometer periodicity," *J. Appl. Phys.* **127**(19), 193104 (2020).
- G. Rosenman, P. Urenski, A. Agronin, Y. Rosenwaks, and M. Molotskii, "Submicron ferroelectric domain structures tailored by high-voltage scanning probe microscopy," *Appl. Phys. Lett.* **82**, 103–105 (2003).
- R. V. Gainutdinov, T. R. Volk, and H. H. Zhang, "Domain formation and polarization reversal under atomic force microscopy-tip voltages in ion-sliced linbo<sub>3</sub> films on SiO<sub>2</sub>/LiNbO<sub>3</sub> substrates," *Appl. Phys. Lett.* **107**, 162903 (2015).
- J. Ma, X. Cheng, N. Zheng, P. Chen, X. Xu, T. Wang, D. Wei, Y. Nie, S. Zhu, M. Xiao, and Y. Zhang, "Fabrication of 100-nm-period domain structure in lithium niobate on insulator," *Opt. Express* **31**, 37464 (2023).
- J. Ma, N. Zheng, P. Chen, X. Xu, Y. Zhu, Y. Nie, S. Zhu, M. Xiao, and Y. Zhang, "Tip-induced nanoscale domain engineering in x-cut lithium niobate on insulator," *Opt. Express* **32**, 14801 (2024).
- H. Zhang, H. Zhu, Q. Li, and H. Hu, "Reversed domains in x-cut lithium niobate thin films," *Opt. Mater.* **109**, 110364 (2020).
- B. Mu, X. Wu, Y. Niu, Y. Chen, X. Cai, Y. Gong, Z. Xie, X. Hu, and S. Zhu, "Locally periodically poled LNOI ridge waveguide for second harmonic generation," *Chin. Opt. Lett.* **19**, 060007 (2021).
- F. Yang, J. Lu, M. Shen, G. Yang, and H. X. Tang, "Symmetric second-harmonic generation in sub-wavelength periodically poled thin film lithium niobate," *Optica* **11**, 1050–1055 (2024).
- C. Xin, K. Pawel, V. Shvedov, K. Koynov, B. Wang, J. Trull, C. Cojocar, W. Krolikowski, and Y. Sheng, "Ferroelectric domain engineering by focused infrared femtosecond pulses," *Appl. Phys. Lett.* **107**, 141102 (2015).
- Y. Sheng, X. Chen, T. Xu, S. Liu, R. Zhao, and W. Krolikowski, "Research progress on femtosecond laser poling of ferroelectrics," *Photonics* **11**, 447 (2024).
- T. Xu, K. Switkowski, X. Chen, S. Liu, K. Koynov, H. Yu, H. Zhang, J. Wang, Y. Sheng, and W. Krolikowski, "Three-dimensional nonlinear photonic crystal in ferroelectric barium calcium titanate," *Nat. Photonics* **12**, 591–595 (2018).
- S. Keren-Zur and T. Ellenbogen, "A new dimension for nonlinear photonic crystals," *Nat. Photonics* **12**, 575–577 (2018).
- Y. Zhang, Y. Sheng, S. Zhu, M. Xiao, and W. Krolikowski, "Nonlinear photonic crystals: From 2D to 3D," *Optica* **8**, 372–381 (2021).
- Y. Sheng, A. Best, H.-J. Butt, W. Krolikowski, A. Arie, and K. Koynov, "Three-dimensional ferroelectric domain visualization by Čerenkov-type second harmonic generation," *Opt. Express* **18**, 16539–16545 (2010).
- Y. Sheng, V. Roppo, K. Kalinowski, and W. Krolikowski, "Role of a localized modulation of  $\chi^{(2)}$  in Čerenkov second-harmonic generation in nonlinear bulk medium," *Opt. Lett.* **37**, 3864–3866 (2012).

- <sup>30</sup>S. M. Saitiel, Y. Sheng, N. Voloch-Bloch, D. N. Neshev, W. Krolikowski, A. Arie, K. Koynov, and Y. S. Kivshar, "Cerenkov-type second-harmonic generation in two-dimensional nonlinear photonic structures," *IEEE J. Quantum Electron.* **45**, 1465–1472 (2009).
- <sup>31</sup>S. M. Saitiel, D. N. Neshev, R. Fischer, W. Krolikowski, A. Arie, and Y. S. Kivshar, "Generation of second-harmonic conical waves via nonlinear Bragg diffraction," *Phys. Rev. Lett.* **100**, 103902 (2008).
- <sup>32</sup>X. Xu, T. Wang, P. Chen, C. Zhou, J. Ma, D. Wei, H. Wang, B. Niu, X. Fang, D. Wu, S. Zhu, M. Gu, M. Xiao, and Y. Zhang, "Femtosecond laser writing of lithium niobate ferroelectric nanodomains," *Nature* **609**, 496–501 (2022).
- <sup>33</sup>O. Yesharim, S. Pearl, J. Foley-Comer, I. Juwiler, and A. Arie, "Direct generation of spatially entangled qudits using quantum nonlinear optical holography," *Sci. Adv.* **9**, 7968 (2023).